Desalination and Water Treatment
www.deswater.com
doi: 10.5004/dwt.2020.25000

179 (2020) 323–331
March

Adsorption of Methyl Green dye onto MCM-41: equilibrium, kinetics and thermodynamic studies

Saja M. Alardhi, Jamal M. Alrubaye, Talib M. Albayati*

Department of Chemical Engineering, University of Technology, Baghdad, Iraq, emails: sajamohsen1987@yahoo.com (S.M. Alardhi), 80046@uotechnology.edu.iq (T.M. Albayati)

Received 10 May 2019; Accepted 7 October 2019

ABSTRACT

The nanoporous material, Mobil Composition of Matter No. 41 (MCM-41), was prepared and characterized in order to adsorb methyl green (MG) dye from artificial wastewater by adsorption method. The MCM-41 was characterized through X-ray diffraction spectroscopy, scanning electron microscopy, Fourier transform infrared spectroscopy and Brunauer–Emmett–Teller. The preliminary results were examined for adsorbent mesoporous material samples, in order to estimate the best states for the adsorption of the model dye: adsorbent dose (0.00–80.04 g) contact time (8–150 min), temperature (25°C–45°C), and initial concentration of dye (10–50 mg/L) where the removal efficiency of MG dye under optimum conditions was around 99%. The outcomes were elucidating that the adsorption isotherms can be quite befitting by the Temkin model, with a coefficient of determination 0.9669. The adsorption kinetics of MG onto adsorbate was strongly represented by a pseudo-second-order kinetic model.

Keywords: MCM-41; Methyl green, Adsorption; Isotherm models; Kinetics; Thermodynamic; Wastewater treatment

1. Introduction

More than 10,000 dyes are commercially accessible and widely used in different industrial sectors, including pulp and paper construction, dyeing of textiles, clothes, printing, leather processing and food industries [1]. There are various approaches for dyes classifications. It can be divided in terms of composition, color and applying means [2]. Cationic triphenylmethane dyes are widespread in industry and biomedical applications as bacterial antigens. Methyl green (MG) [$C_{27}H_{35}BrClN_3 \cdot ZnCl_2$] is a basic triphenylmethane-type dicationic dye, commonly employed to change the solutions colors in biology and medicine plus as a photochromophore to excite coagulated films [3]. Its molecular structure is depicted in Fig. 1.

Now notable consideration has been united on the expulsion of the effluents-containing dyes having inherent toxicity. Different modes for dye elimination were selected in order to limit their drastic effect on the environment. These techniques include ozonation, coagulation–flocculation, microbial decomposition, photo-catalytic decolonization, sono-chemical, filtration and membrane separation, liquid–liquid extraction, wet air oxidation, electrochemical methods and adsorption. Amongst different ways of dye rejection, it can be noted that the common powerful approach that affords promising results is adsorption [4,5]. Adsorbents employed for water remediation are either of the natural source or the outcome of an industrialized production and/or activation method. Conventional natural adsorbents are natural zeolites, clay minerals, biopolymers or oxides. After the invention of M41S silica in 1992, mesoporous substances such as MCM-41, MCM-48 and SBA-15 have brought serious regard due to their great surface areas, non-toxicity, well-defined pore constructions, biocompatibility and inert framework [6].

* Corresponding author.

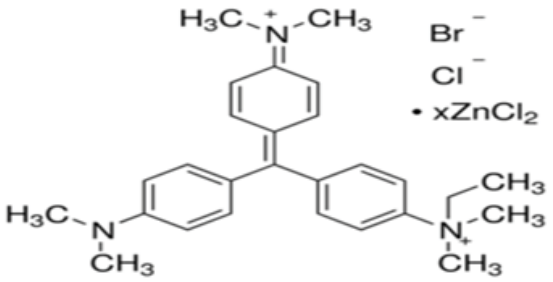

Fig. 1. Molecular structure of methyl green.

The ordered mesoporous molecular sieve MCM-41 with pore diameters between 20 Å and 500 Å [7]. The unique features of the high inner surface area, controllable size of the pore and desirable unity has been considerably applied in materials science, chemistry, physics and other related areas. This innovative mesoporous solid is an excellent catalyst, hosts of quantum structures, shape/size selective adsorbents and catalyst supports [8]. Hexagonal MCM-41 substances have proved their potential affinity toward organic compounds. Recent studies associated with the adsorption of organic particles explained the application of MCM-41 with surfactant. It has been evident that the presence of surfactant cationic substance in the MCM-41 results in alterations not only in porosity but also in surface chemistry of the adsorbent, which in turn controlled their performance as adsorbents [9]. A number of studies used mesoporous materials in different fields such as drug delivery systems [10], catalysis [11], separation process [12] and also used to treat dyes from wastewater effluents [13,14].

In the present study, the Methyl Green (MG) model dye was treated using MCM-41 after its characterization, then the effect of the different variables on the treatment by adsorption process was studied, including the impact of adsorbent dose, contact time, temperature and initial concentration of dye. Isotherm, kinetics and thermodynamic investigations were carried out to estimate the governing mechanisms of the adsorption process. MCM-41 mesoporous nanomaterial has already been applied for the removal of many kinds of contaminants from wastewater. However, there is little research reporting the adsorption and separation of Methyl Green (MG) from aqueous solution by MCM-41. It is acquiring special recognition and considers as a promising alternative to conventional water treatment in textile industries.

2. Materials and methods

2.1. Chemicals

Methyl green (MG) $C_{27}H_{35}BrClN_3{\cdot}ZnCl_2$, cetyltrimethyl ammonium bromide (CTAB, 99%), tetraethyl orthosilicate (TEOS, 98%), sodium hydroxide (NaOH), ethanol (EtOH, 99%) and citric acid ($C_6H_8O_7$) were purchased from Sigma-Aldrich (Germany).

2.2. MCM-41 mesoporous preparation

The preparation procedure involves dissolving 0.34 g of sodium hydroxide and 1.01 g of cetyltrimethyl ammonium bromide in 30 mL distilled water, the solution was then left for 1 h with constant mixing and at room temperature, under static hydrothermal conditions the prepared solution was blend for 4 d at 110°C in a batch autoclaved reactor, The resulting material was filtered and washed with distilled water and ethanol, after that left to dry in air at 25°C [8].

2.3. Characterization

The crystalline structure of the prepared mesoporous material was characterized by the X-ray diffraction (XRD) device (XRD-6000, Shimadzu, Japan), the X-ray source emits radiation at 0.15405 nm wavelength. The system operates at 80 mA emission current and 60 kV.

The macrospores composition was identified by scanning electron microscopy (Tescan VEGA 3 SB, SEM). The chemical composition analysis of MCM-41, (FT-IR, infrared spectra) was used. The specific surface area of the samples was checked by Brunauer–Emmett–Teller device (Type: Q-surf 9600, Origin: USA).

2.4. Batch MG adsorption

The stock solution was made by dissolving 1 g of MG dye in 1 L of distilled water to produce 1,000 ppm. Batch adsorption tests were performed by adding the desired amounts of MCM-41 to 50 mL of MG dye solution (10–50 ppm) and solution pH equals 6. Then, the mixture had settled in an electrical shaker (Type: BS-21, Heidolph Origin: Germany) set at 250 rpm and a desired temperature 25°C–45°C where the contact time is 15–80 min. After the end of each run, spent MCM-41 was centrifuged, filtered, and then the filtrate was collected for residual MG concentration measurement. The concentration of MG was determined at a maximum wavelength of 630 nm by UV–Vis spectrophotometer (Type: U.V-1100, Origin: China). The adsorbed amount per gram of MCM-41 (mg/g) or the adsorption capacity (q), was achieved using the following equation [15]:

$$q_e = \frac{\left(C_i - C_f\right)V}{M} \tag{1}$$

where q_e is the adsorption capacity at equilibrium (mg/g), C_i and C_f (mg/L) are the initial and final concentrations, respectively, V (L) is the solution volume, and M (g) is the amount of MCM-41 used.

The dye removal ratio was calculated using the equation [16]:

$$\%\text{Removal} = \frac{C_i - C_e}{C_i} \times 100 \tag{2}$$

where C_e is the concentration of adsorbate at the equilibrium (mg/L).

2.5. Adsorption isotherm model

2.5.1. Langmuir isotherm

This model assumes the formation of monolayer adsorption with equal heat of adsorption on the surface [17]. The linearization form is shown as follows [18]:

$$\frac{C_e}{q_e} = \frac{1}{q_{\max}} C_e + \frac{1}{q_{\max} b} \quad (3)$$

where $q_{\max}$: Langmuir constant associating to adsorption capacity (mg/g), b: constant refers to energy of adsorption (L/mg).

The constants $q_{\max}$ and b can be calculated from Eq. (3) by the slope of the linear plot of C_e/q_e vs. C_e. Moreover, the dimensionless equilibrium parameter R_L shows the isotherm is favorable, unfavorable, irreversible or linear when the value of $R_L < 1$, $R_L > 1$, $R_L = 0$ and $R_L = 1$, respectively. It is expressed by Eq. (4) as follows:

$$R_L = \frac{1}{1 + bC_i} \quad (4)$$

2.5.2. Freundlich isotherm

The depiction of the surface energy is accomplished using the equation given by [19]:

$$\ln q_e = \ln K_f + \frac{1}{n} \ln C_e \quad (5)$$

where K_f: constant related to adsorption capacity of the sorbent; n: adsorption intensity based on the value of n, the poor adsorption, moderate adsorption, and good characteristics have been found when the value of $n < 1$, $n = 1–2$, and $n = 2–10$, respectively [20].

2.5.3. Temkin isotherm

The linearized form of Temkin isotherm model is expressed as:

$$q_e = B \ln K_t + B \ln C_e \quad (6)$$

where K_t is the equilibrium binding constant (L/g) corresponding to the maximum binding energy, $B = (RT/b)$ is a Temkin constant (J/kJ), b is the heat of adsorption (kJ/mol), R is the universal gas constant (8.314 J/mol K), and T is absolute temperature (K).

3. Results and discussion

3.1. Characterization of adsorbents

The crystalline construction, structural character and phase structure of the manufactured MCM-41 elements were analyzed by XRD (Type: Shimadzu-6000, Origin: Japan). X-ray diffractometer with 2θ range from 0° to 10° with scan rate 2 (deg/min) and Cu-kα (λ = 1.541) as radiation source was applied (Fig. 2a). The small-angle XRD pattern shows characteristic diffraction peaks for MCM-41. A strong diffraction peak for 100 plane at 2.8 indicates the mesoporosity and existence of a periodic hexagonal long range order of the channel [6].

Morphology analysis of MCM-41 was conducted using SEM instrument (Type: VEGA 3 LM, Origin: Germany) (Fig. 2b). The SEM image of MCM-41 clearly demonstrates the well-ordered hexagonal array construction. Closer scoping on the surface of the MCM-41 assures the presence of mesoporous uniform size channels with a sphere shape, puffy or swollen structures and smooth surfaces in the range of 5–100 nm in diameter, similar results have been reported by Farjadian et al. [21]. These swollen structures are preferable for absorption of contaminated dye. A narrow pore configuration can also be recognized from the micrographs.

Fig. 2c shows the FTIR spectrum of the MCM-41. For MCM-41, the peaks around 1,024 and 1,193 cm^{-1} are assigned to the asymmetric stretching of Si–O–Si groups. Furthermore, broad and weak bands at 960 and 958 cm^{-1} are indexed to the symmetric stretching vibration of Si–OH moieties presented in the pore channels. The broad peak around 3,446 to 3,221 cm^{-1} is marked for Si–OH; moreover, O–H bending peaks are present at 1,641 and 1,639 cm^{-1}. The absorption bands at 489 to 433 cm^{-1} were corresponding to the bending vibration of Si–O–Si. The absorption band at 1,481 and 1,483 cm^{-1} indicates C–H stretching vibration of alkyl group. The Brunauer–Emmett–Teller (BET) surface area, pore volume, pore diameter of MCM-41 sample were measured and the results are summarized in Table 1.

3.2. Removal of MG dye

3.2.1. Effect of pH

The chemical characteristics of both adsorbent and adsorbate may vary with pH. The pH of the solution affects the degree of ionization and speciation of various dyes which subsequently leads to a change in the reaction kinetics and equilibrium characteristics of the adsorption process [9]. The value of pH for the pre-treatment solution without any additives was equal to 6 in order to study the effect of the pH on the dye removal. Then different solutions having different values of pH were prepared and adjusted from 2 to 12 by using sodium hydroxide (NaOH) and citric acid ($C_6H_8O_7$) as shown in Fig. 3. It is clear from this figure that when pH exceeds 8, the color of the solution changes from blue to approximately colorless, even with the absence of sorbent. This is an indication of the interaction between the dye solution and alkali solution; therefore, the pH was set to be unchanged for subsequent experiments. In particular if the surface charge density is low, only the influence of the pH value on the adsorbate properties has to be considered [22].

3.2.2. Effect of adsorbent dose

Effect of adsorbent dose on MG adsorption is shown in Fig. 4. It can be observed that as the adsorbent dose increased from 0.008 to 0.02 g, the removal efficiency increased from 85% to 99%, respectively. These results can be interpreted in terms of an increase in the availability of binding sites occurs, and consequently reflected in the adsorption capacity [23]. No notable advance in dye removal was noticed using more than 0.02 g of the adsorbent dosage where the molecules are clustered into active sites which minimize MCM-41 available surface area.

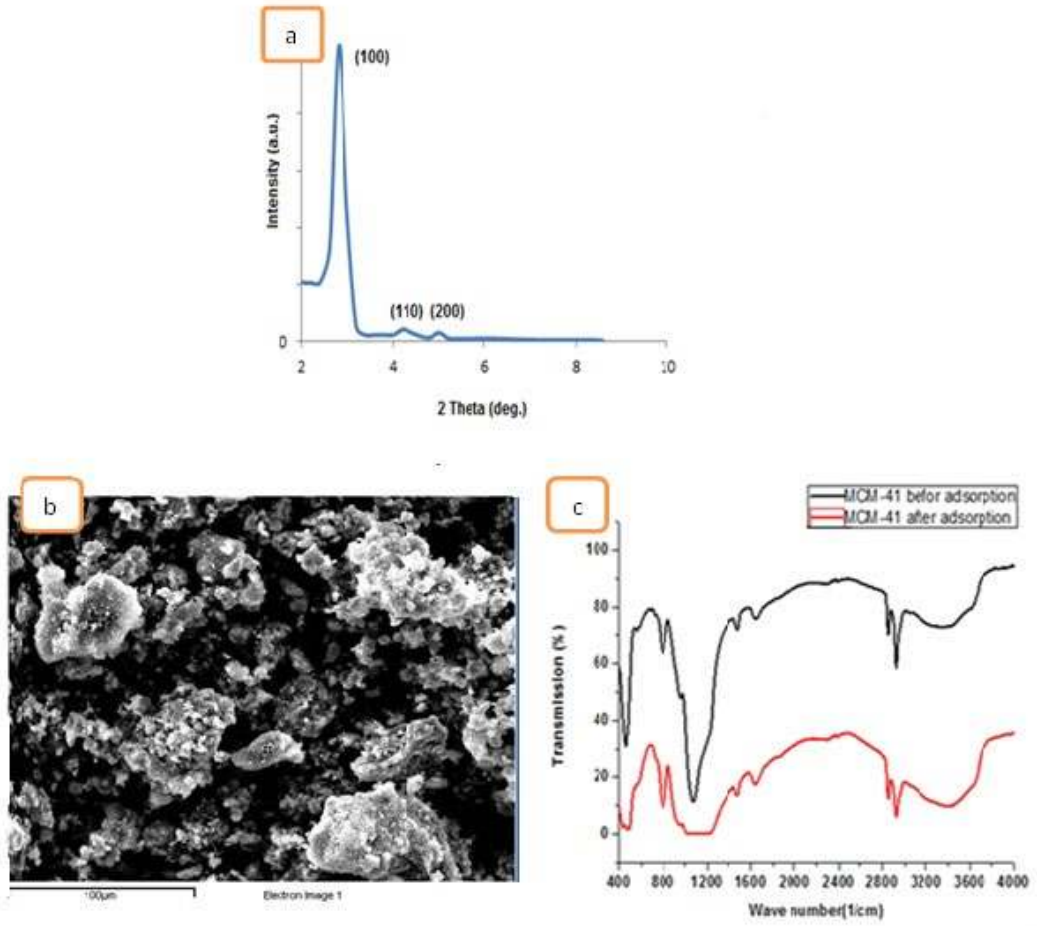

Fig. 2. (a) XRD pattern of the synthesized MCM-41 nano adsorbent, (b) scanning electron microscopic (SEM) images of MCM-41 specimen powder and (c) FT-IR spectra of MCM-41 before and after adsorption of dye.

Table 1
Physicochemical properties of MCM-41

Sample	d_{100} (nm)	a_0 (nm)	S_{BET} (m^2/g)	V_p (cm^3/g)	D_{BJH} (nm)	W_t (nm)	μ_p (cm^3/g)
MCM-41	3.35	3.868	1,500	0.7	2.5	1.37	0.6

3.2.3. Effect of contact time

The results obtained by testing the effect of contact time on the adsorption performance of MG are presented in Fig. 5. The results showed that adsorption rate was relatively high at the beginning of the experiment which can be attributed to the availability of active sites for MG adsorption, the previously mentioned binding sites become limited as the time passed [24]. The adsorption rate gets slower with time due to the equilibrium state occurs at 60 min, followed by a plateau up until the end of the experiment.

3.2.4. Effect of initial dye concentration

It is of the essence to study the effect of varying the initial concentration of MG due to the fact that for a certain adsorbent amount, only limited adsorbate concentration can be adsorbed [25]. Initial MG concentrations ranging from 10 to 50 ppm were tested. Fig. 6 shows that the removal efficiency of the initial MG concentration was the higher range of the studied concentration 10 and 20 mg/L and almost equilibrium, the ability of the sorbent MCM-41 to remove the dye was lower, while as the initial concentrations increased from 30 to 50 mg/L, the removal efficiency decreased. The reason can be due to an increase in the driving force of the concentration gradient happens as the initial concentration increases [26].

3.2.5. Effect of temperature

In order to ascertain the extent of temperature effect on MG adsorption capacity using MCM-41, the recent work examined the effect of 25°C, 35°C and 45°C. It can be concluded from Fig. 7, that there is no significant and noticeable difference in the adsorption capacities by applying

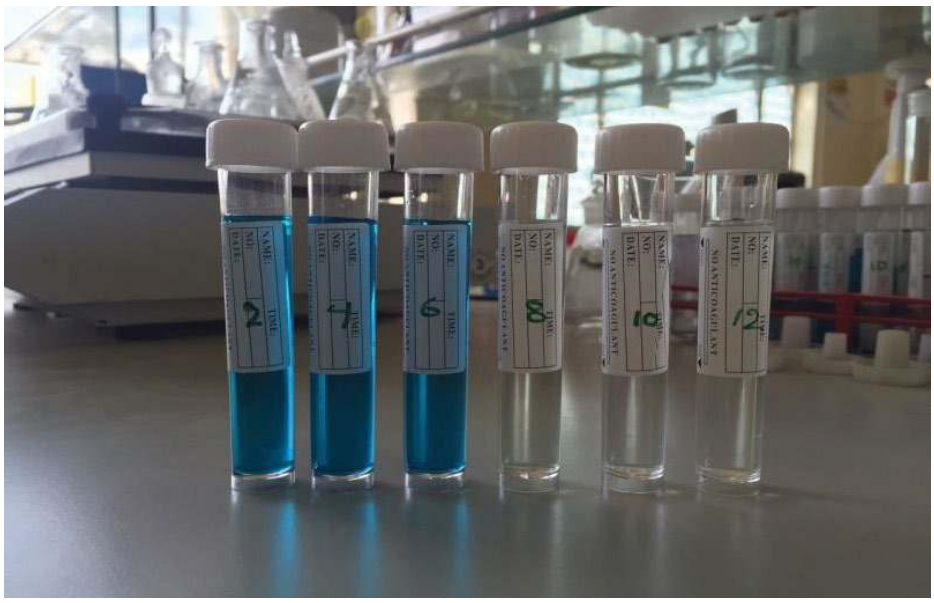

Fig. 3. Effect of pH on MG removal (concentration of dye = 20 mg/L, contact time = 60 min, temperature = 25°C).

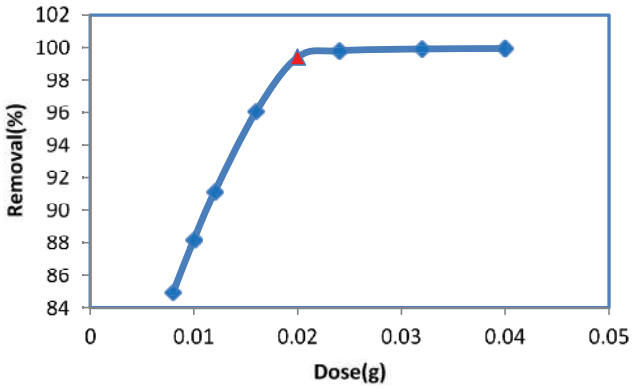

Fig. 4. Effect of adsorbent dose on MG removal (concentration of dye = 20 mg/L, contact time = 60 min, pH = 6, temperature = 25°C).

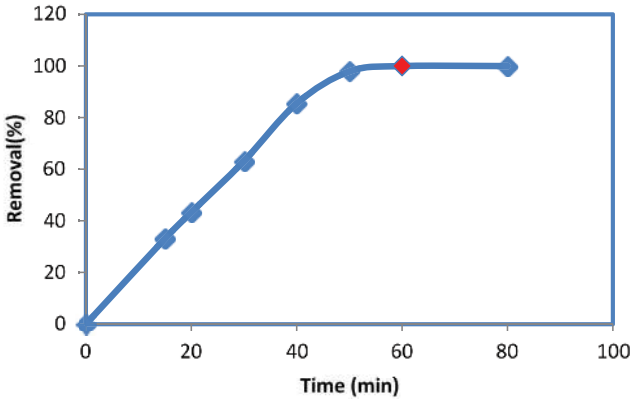

Fig. 5. Effect of contact time on MG removal (concentration of dye = 20 mg/L, adsorbent dose = 0.02 g, pH = 6, temperature = 25°C).

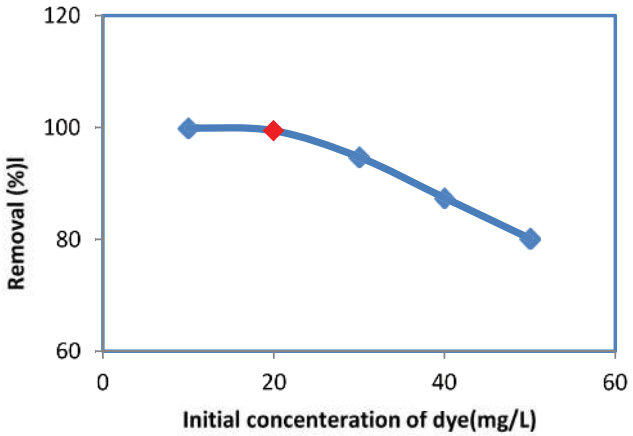

Fig. 6. Effect of initial dye concentration on adsorption of MG (adsorbent dose = 0.02 g, contact time = 60 min, pH = 6, temperature = 25°C).

the three suggested temperatures, with 99.4%, 99.45% and 99.45%, respectively. The latter system behavior minimizes the necessity of temperature control, and hence enhances the system's economical aspect. These results are in agreement with Bhattacharyya and Sharma [27].

3.2.6. Adsorption isotherm models

The equilibrium adsorption data were fitted into Langmuir, Freundlich and Temkin isotherms. For each isotherm, the equilibrium capacities, rate constants and related correlation coefficients are shown in Figs. 8a–c. As presented in Table 2, Temkin isotherm offered the highest regression coefficient (R^2 = 0.9669). In Temkin isotherm, the heat of adsorption of all the molecules in the layer reduces linearly with covering due to adsorbent–adsorbate interactions.

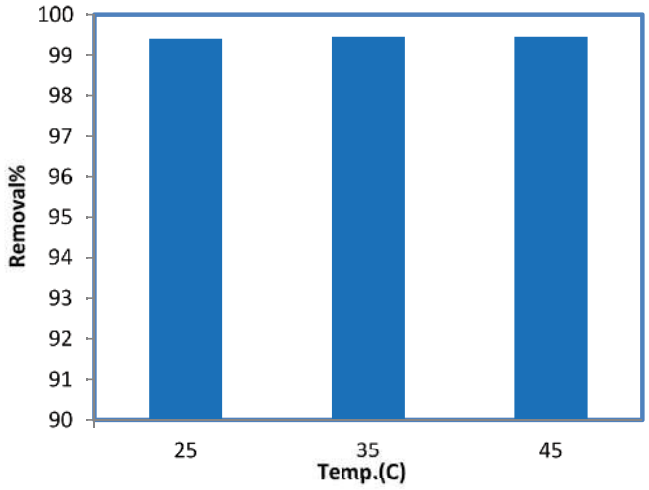

Fig. 7. Effect of temperature on MG removal (adsorbent dosage = 0.02 g, contact time = 60 min, pH = 6, concentration of dye = 20 mg/L).

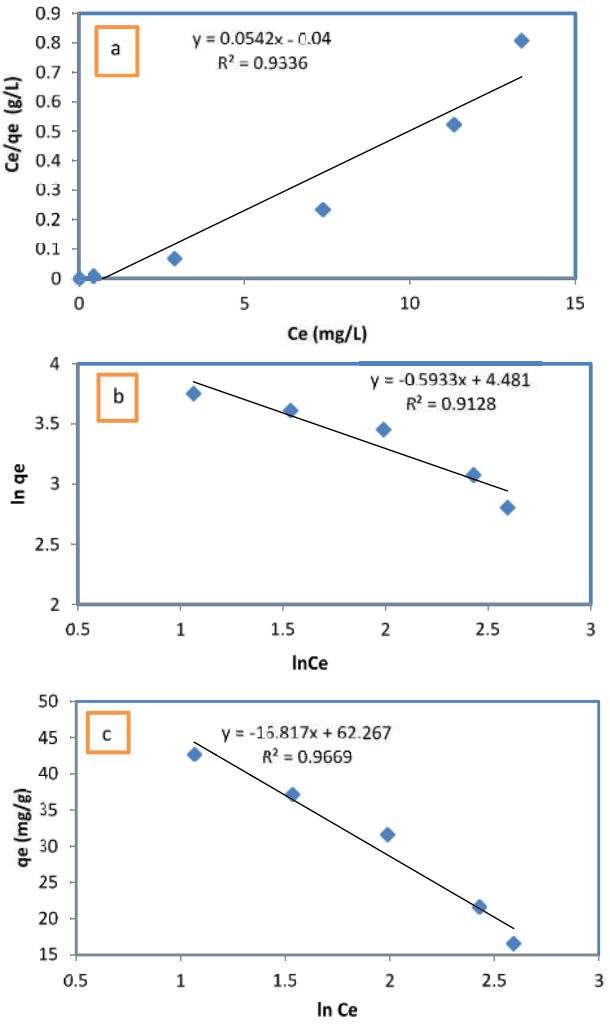

Fig. 8. (a) Langmuir model, (b) Freundlich model and (c) Temkin model for MG adsorption.

This model assumes that adsorption is described by a regular distribution of binding energies in the layer, up to a certain maximum binding energy [24,26]. Furthermore, from the experimental data calculated in Table 2. For Langmuir isotherm, the R_L value is greater than 0 but less than 1 indicating that Langmuir isotherm was also favorable, the maximum monolayer coverage capacity q_{max} = 18.45 mg/g with correlation coefficient R^2 = 0.9336.

3.3. Adsorption kinetics

The rate constant of adsorption is determined by the following first order rate expression:

$$\log\left(q_e - q_t\right) = \log q_e - \left(\frac{K_1}{2.303}t\right) \tag{7}$$

where q_t; is the quantity of dye adsorbed at time t (min) and K_1 is pseudo-first-order of the adsorption rate constant.

The pseudo-second-order equation is based on the following equation:

$$\frac{t}{q_t} = \frac{1}{K_2 q_e^2} + \frac{1}{q_e} \times t \tag{8}$$

where K_2 is the pseudo-second-order rate constant for adsorption (g/mg min), which can be estimated by plotting t/q_t vs. t. The possibility of film or intraparticle diffusion was explored by using the Weber–Morris model:

$$q_t = K_p t^{0.5} + I \tag{9}$$

where K_p is intraparticle diffusion rate constant (mg/g min$^{0.5}$); I is the intraparticle diffusion constant. Table 3 and Figs. 9a–c represents the kinetic parameters of the three suggested kinetic models. The correlation coefficient of the second order kinetic model (0.9835) is relatively higher than that resulted from the first-order kinetic model (0.8966). The previously mentioned results were confirmed the rate-limiting step, with valence forces activity throughout the replacement or sharing of electrons [27]. If the linear portion of the intraparticle diffusion kinetic plot does not pass through the origin, then some extent of boundary layer control is involved, and that intraparticle diffusion is not the single rate controlling step, but additional processes are also controlling the rate of sorption. The latter explanation fits well the plot in Fig. 9c [28].

3.4. Adsorption thermodynamics

Thermodynamic parameters were evaluated to determine the free energy change ($\Delta G°$), enthalpy change ($\Delta H°$) and entropy change ($\Delta S°$) by using the following:

Gibbs free energy change [29]:

$$\Delta G° = -RT \ln K_C \tag{10}$$

where R is universal gas constant (8.314 J/mol K) and T is the absolute temperature in K. The apparent equilibrium constant (K_C) of the adsorption is defined as follows:

Table 2
Parameters of isotherm models

Langmuir				Freundlich			Temkin		
q_{max}	R_L	b	R^2	K_f	n	R^2	b	K_t	R^2
18.45	0.035	1.355	0.9336	88.322	1.685	0.9128	0.147	1.31	0.9669

Table 3
Kinetic models for the sorption of MG onto MCM-41

Pseudo-first-order			Pseudo-second-order			Intraparticle diffusion		
q_e (mg/g)	K_1 (min^{-1})	R^2	q_e (mg/g)	K_2 (g/mg min)	R^2	I	K_p (mg/g min$^{0.5}$)	R^2
196.38	0.0944	0.8966	285.7	0.000014	0.9835	8.9594	7.383	0.894

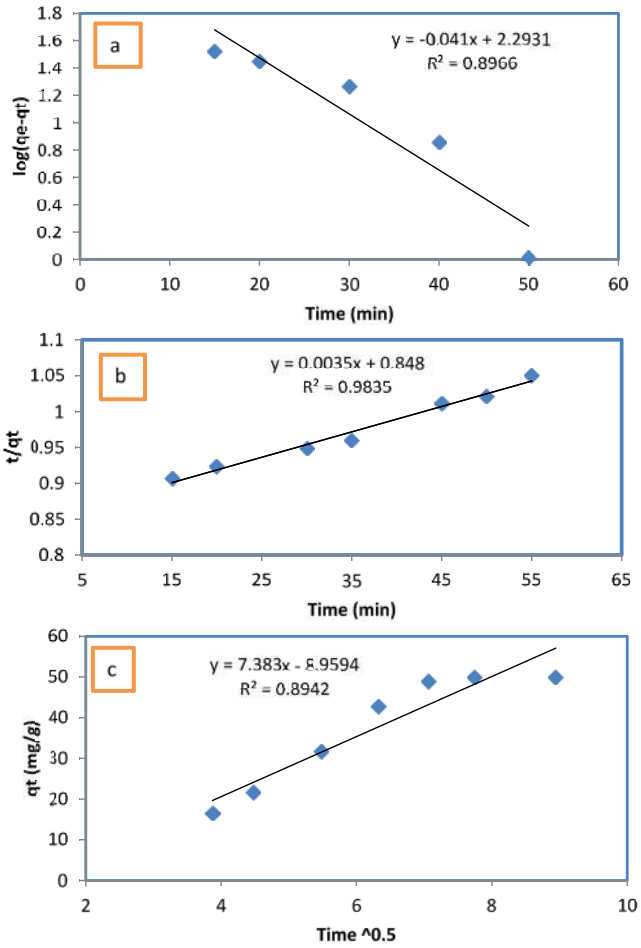

Fig. 9. (a) Pseudo-first-order kinetic plot for MG adsorption, (b) pseudo-second-order kinetic plot or MG adsorption and (c) intraparticle diffusion plot for MG adsorption.

$$K_C = \frac{q_e}{C_e} \tag{11}$$

In this case, the activity should be used instead of concentration in order to obtain the standard thermodynamic equilibrium constant (K_C) of the adsorption system.

$$\Delta G^\circ = \Delta H^\circ - T\Delta S^\circ \tag{12}$$

$$\ln K_C = \frac{\Delta S^\circ}{R} - \frac{\Delta H^\circ}{RT} \tag{13}$$

where ΔH° and ΔS° (J/mol) are resulted from the slope and intercept of Van't Hoff scheme of $\ln K_C$ vs. $1/T$ Eq. (13). The experimental results of thermodynamic parameters for the sorption of MG using MCM-41 are presented in Table 4. The positive value of (ΔH°) assures that the adsorption of MG onto MCM41 is an endothermic reaction. Therefore, physical sorption is described by a slight change in enthalpy, typically in the range –10 to –40 kJ/mol (heats of sorption of 10–40 kJ/mol), whereas heat of chemisorption is rarely less than 80 kJ/mol and often exceeds 400 kJ/mol [30,31]. ΔG° must always be negative for a method to be thermodynamically acceptable [32]. The negative values of ΔG° are signs of the spontaneous nature of the sorption system. The increase in ΔG° with an increase in temperature records that the sorption favorable at low temperatures.The positive value of ΔS° verifies randomness increasing at the adsorbate-solution interface during the process of adsorption process [16].

3.5. Batch regeneration system

To investigate the performance of the MCM-41 sorbent, reuse experiments were carried out. At the end of the sorption process, the saturated sorbent was separated by filtration, and then regenerated by shaking in 0.1 M NaOH solution, followed by centrifugation, washing and drying at 70°C. The regenerated adsorbent was reused in subsequent run under the same conditions. Fig. 10 shows the regenerated and recycled results of MCM-41. It indicated that the removal percentage of MG declined by about 2.4% in the first reuse of MCM-41, and decreased slightly in the third cycle. This may be due to the loss of some of the surfactant template from the MCM-41 during regeneration leading to subsequent loss of adsorption. As a result, the MCM-41 adsorbent could be recycled several times.

3.6. Comparative study

The comparison between the MCM-41 with other adsorbents, which is reported in the literature, is shown in Table 5. This table provides useful information about how efficient

Table 4
Thermodynamic parameters for the sorption of MG onto MCM-41

Temperature (K)	$\Delta H°$ (kJ/mol)	$\Delta G°$ (J/mol)	$\Delta S°$ (J/mol K)
298	3.496	–14.929	61.9
308		–15.653	
318		–16.16	

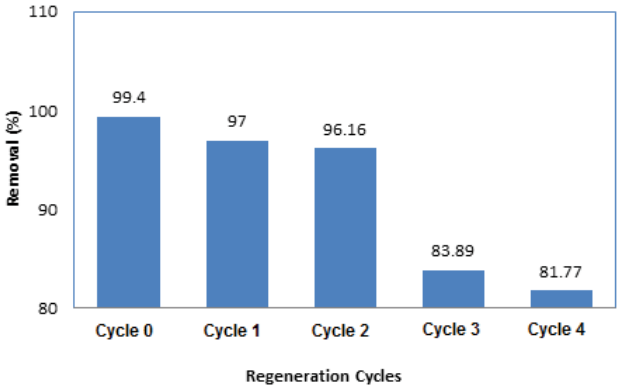

Fig. 10. Reusability of MCM-41 in batch experiment (pH = 6, adsorbent dose = 0.02 g, contact time = 60 min, concentration of dye = 20 mg/L).

Table 5
Adsorption capacities of MG by various adsorbents

No.	Adsorbents	Adsorption capacity Q_{max} (mg g^{-1})	Reference
1	Graphite oxide	29.42	[33]
2	Graphene oxide	28.5	[34]
3	Bamboo	15.5	[35]
5	MCM-41	285.7	This study

MCM-41 adsorbent can enhance the adsorption capacity of MG from other adsorbents materials. It can be noted from Table 5 that MCM-41 is a good adsorbent to remove MG dye because it has a high surface area reach to 1,500 m^2/g compared with the other adsorbents.

4. Conclusions

The adsorption of methyl green from aqueous solutions was performed using the adsorbent MCM-41. The results confirmed that MCM-41 is a promising adsorbent material for the treatment of contaminated dyes wastewater in ambient temperatures. The adsorption efficiency is strongly dependent on the adsorbent dose, contact time and initial dye concentration. The highest removal efficiency was obtained at 0.02 g of MCM-41, 60 min and 20 ppm, respectively. Furthermore, the obtained results showed that temperature did not offer significant effect on process efficiency. Adsorption parameters determined from Langmuir, Freundlich and Temkin isotherms are valuable for the analysis of adsorption mechanisms shown by the stable linear regression coefficient values. For the given experimental conditions, the capacity of the MCM-41 for MG removal was 285.7 mg/g, which may be associated to the structural features of the tested dye and to the nature of their interaction with the surface of MCM-41. The adsorption kinetic data were well illustrated by pseudo-second-order kinetic model. Thermodynamic studies confirmed that the adsorption method is endothermic and spontaneous.

Acknowledgments

The authors gratefully acknowledge financial support from the Nanotechnology Advanced Material Research Center and Department of Chemical Engineering, University of Technology, Baghdad, Iraq.

References

[1] T.M. Albayati, A.A. Sabri, R.A. Alazawi, Separation of methylene blue as pollutant of water by SBA-15 in a fixed-bed column, Arab. J. Sci. Eng., 41 (2016) 2409–2415.
[2] M.T. Yagub, T.K. Sen, S. Afroze, H.M. Ang, Dye and its removal from aqueous solution by adsorption: a review, Adv. Colloid Interface Sci., 209 (2014) 172–184.
[3] A. Nezamzadeh-Ejhieh, Z. Shams-Ghahfarokhi, Photodegradation of methyl green by nickel-dimethylglyoxime/ZSM-5 zeolite as a heterogeneous catalyst, J. Chem., 2013 (2013) 11.
[4] D. Pathania, S. Sharma, P. Singh, Removal of methylene blue by adsorption onto activated carbon developed from *Ficus carica* bast, Arab. J. Chem., 10 (2017) S1445–S1451.
[5] T.M. Albayati, G.M. Alwan, O.S. Mahdy, High performance methyl orange capture on magnetic nanoporous MCM-41 prepared by incipient wetness impregnation method, Korean J. Chem. Eng., 34 (2017) 259–265.
[6] J.S. Beck, J.C. Vartuli, W.J. Roth, M.E. Leonowicz, C.T. Kresge, K.D. Schmitt, C.T.W. Chu, D.H. Olson, E.W. Sheppard, S.B. McCullen, J.B. Higgins, J.L. Schlenker, A new family of mesoporous molecular sieves prepared with liquid crystal templates, J. Am. Chem. Soc., 114 (1992) 10834–10843.
[7] S. Bhattacharyya, G. Lelong, M.L. Saboungi, Recent progress in the synthesis and selected applications of MCM-41: a short review, J. Exp. Nanosci., 1 (2006) 375–395.
[8] H. Chen, Y. Wang, Preparation of MCM-41 with high thermal stability and complementary textural porosity, Ceram. Int., 28 (2002) 541–547.
[9] B. Boukoussa, R. Hamacha, A. Morsli, A. Bengueddach, Adsorption of yellow dye on calcined or uncalcined Al-MCM-41 mesoporous materials, Arab. J. Chem., 10 (2017) S2160–S2169.
[10] T.M. Albayati, A.A. Jassam, Synthesis and characterization of mesoporous materials as a carrier and release of prednisolone in drug delivery system, J. Drug Deliv. Sci. Technol., 53 (2019) 101176.
[11] T.M. Albayati, S.E. Wilkinson, A.A. Garforth, A.M. Doyle, Heterogeneous Alkane Reactions over Nanoporous Catalysts, 11-Transp Porous Media, Volume 104, 2014, pp. 315–333.
[12] T.M. Albayati, A.M. Doyle, Purification of aniline and nitrossubstituted aniline contaminants from aqueous solution using beta zeolite, Bulg, J. Sci. Educ., 23 (2014) 105–114.
[13] T.A. Arica, E. Ayas, M.Y. Arica, Magnetic MCM-41 silica particles grafted with poly (glycidylmethacrylate) brush: modification and application for removal of direct dyes, Microporous Mesoporous Mater., 243 (2017) 164–175.
[14] C.-K. Lee, S.-S. Liu, L.-C. Juang, C.-C. Wang, K.-S. Lin, M.-D. Lyu, Application of MCM-41 for dyes removal from wastewater, J. Hazard. Mater., 147 (2007) 997–1005.
[15] C.B. Vidal, A.L. Barros, C.P. Moura, A.C. De Lima, F.S. Dias, L.C. Vasconcellos, P.B. Fechine, R.F. Nascimento, Adsorption of polycyclic aromatic hydrocarbons from aqueous solutions by

modified periodic mesoporous organosilica, J. Colloid Interface Sci., 357 (2011) 466–473.
[16] A. Darwish, M. Rashad, H.A. AL-Aoh, Methyl orange adsorption comparison on nanoparticles: isotherm, kinetics, and thermodynamic studies, Dyes Pigm., 160 (2019) 563–571.
[17] K.Y. Foo, B.H. Hameed, Insights into the modeling of adsorption isotherm systems, Chem. Eng. J., 156 (2010) 2–10.
[18] I. Langmuir, The constitution and fundamental properties of solids and liquids. II. Liquids, J. Am. Chem. Soc., 39 (1917) 1848–1906.
[19] A.A. Sabri, T.M. Albayati, R.A. Alazawi, Synthesis of ordered mesoporous SBA-15 and its adsorption of methylene blue, Korean J. Chem. Eng., 32 (2015) 1835–1841.
[20] Y. Yao, H. Bing, X. Feifei, C. Xiaofeng, Equilibrium and kinetic studies of methyl orange adsorption on multiwalled carbon nanotubes, Chem. Eng. J., 170 (2011) 82–89.
[21] F. Farjadian, P. Ahmadpour, S.M. Samani, M. Hosseini, Controlled size synthesis and application of nanosphere MCM-41 as potent adsorber of drugs: a novel approach to new antidote agent for intoxication, Microporous Mesoporous Mater., 213 (2015) 30–39.
[22] T.M. Albayati, K.R. Kalash, Polycyclic aromatic hydrocarbons adsorption from wastewater using different types of prepared mesoporous materials MCM-41 in batch and fixed bed column. Process Saf. Environ. Prot., 133 (2020) 124–136.
[23] M.A.M. Salleh, D.K. Mahmoud, W.A.W.A. Karim, A. Idris, Cationic and anionic dye adsorption by agricultural solid wastes: A comprehensive review, Desalination, 280 (2011) 1–13.
[24] S.H. Azaman, A. Afandi, B. Hameed, A.M. Din, Removal of Malachite Green from aqueous phase using coconut shell activated carbon: adsorption, desorption, and reusability studies, J. Appl. Sci. Eng., 21 (2018) 317–330.
[25] S. Banerjee, M.C. Chattopadhyaya, Adsorption characteristics for the removal of a toxic dye, tartrazine from aqueous solutions by a low cost agricultural by-product, Arab. J. Chem., 10 (2017) S1629–S1638.
[26] J. Iqbal, F.H. Wattoo, M.H.S. Wattoo, R. Malik, S.A. Tirmizi, M. Imran, A.B. Ghangro, Adsorption of acid yellow dye on flakes of chitosan prepared from fishery wastes, Arab. J. Chem., 4 (2011) 389–395.
[27] K.G. Bhattacharyya, A. Sharma, Kinetics and thermodynamics of Methylene Blue adsorption on Neem (*Azadirachta indica*) leaf powder, Dyes Pigm., 65 (2005) 51–59.
[28] S. Svilović, D. Rušić, R. Stipišić, Modeling batch kinetics of copper ions sorption using synthetic zeolite NaX, J. Hazard. Mater., 170 (2009) 941–947.
[29] M.L.F.A. De Castro, M.L.B. Abad, D.A.G. Sumalinog, R.R.M. Abarca, P. Paoprasert, M.D.G. de Luna, Adsorption of Methylene Blue dye and Cu(II) ions on EDTA-modified bentonite: isotherm, kinetic and thermodynamic studies, Sustain. Environ. Res., 28 (2018) 197–205.
[30] M.J.P. Brito, C.M. Veloso, L.S. Santos, R.C.F. Bonomo, R.d.C.I. Fontan, Adsorption of the textile dye Dianix® royal blue CC onto carbons obtained from yellow mombin fruit stones and activated with KOH and H_3PO_4: kinetics, adsorption equilibrium and thermodynamic studies, Powder Technol., 339 (2018) 334–343.
[31] M. Preuss, W. Schmidt, F. Bechstedt, Coulombic amino group-metal bonding: adsorption of adenine on Cu (110), Phys. Rev. Lett., 94 (2005) 236102.
[32] U. Etim, S. Umoren, U. Eduok, Coconut coir dust as a low cost adsorbent for the removal of cationic dye from aqueous solution, J. Saudi Chem. Soc., 20 (2016) S67–S76.
[33] A.A. Farghali, M. Bahgat, W.M.A. El Rouby, M.H. Khedr, Preparation, decoration and characterization of graphene sheets for methyl green adsorption, J Alloys Compd., 555 (2013) 193–200.
[34] P. Sharma, B.K. Saikia, M.R. Das, Removal of methyl green dye molecule from aqueous system using reduced graphene oxide as an efficient adsorbent: kinetics, isotherm and thermodynamic parameters, Colloids Surf., A, 457 (2014) 125–133.
[35] A. Adnan Atshan, Adsorption of methyl green dye onto bamboo in batch and continuous system, Iraqi J. Chem. Petrol. Eng., 15 (2014) 65–72.